



Methane paradox in tropical lakes? Sedimentary fluxes rather than water column production in oxic waters sustain methanotrophy and emissions to the atmosphere

5 Cédric Morana^{1,2*}, Steven Bouillon¹, Vimac Nolla-Ardèvol¹, Fleur A.E. Roland², William Okello³, Jean-Pierre Descy², Angela Nankabirwa³, Erina Nabafu³, Dirk Springael¹, Alberto V. Borges².

¹Department of Earth & Environmental Sciences, KU Leuven, Belgium

²Chemical Oceanography Unit, Université de Liège, Belgium

³Limnology Unit, National Fisheries Resources Research Institute, Uganda

10 *Correspondence to:* Cédric Morana (Cedric.Morana@kuleuven.be)

Abstract. Despite growing evidence that methane (CH₄) formation could also occur in well-oxygenated surface freshwaters, its significance at the ecosystem scale is uncertain. Empirical models based on data gathered at high latitude predict that the contribution of oxic CH₄ increases with lake size and should represent the majority of CH₄ emissions in large lakes. However, such predictive models could not directly apply to tropical lakes which differ from their temperate counterparts in some
15 fundamental characteristics, such as year-round elevated water temperature. We conducted stable isotope tracer experiments which revealed that oxic CH₄ production is closely related to phytoplankton metabolism, and is a common feature in five contrasting African lakes. Nevertheless, methanotrophic activity in surface waters and CH₄ emissions to the atmosphere were predominantly fuelled by CH₄ generated in sediments and physically transported to the surface. Indeed, measured CH₄ bubble dissolution flux and diffusive benthic CH₄ flux were several orders of magnitude higher than CH₄ production in surface waters.
20 Microbial CH₄ consumption dramatically decreased with increasing sunlight intensity, suggesting that the freshwater “CH₄ paradox” might be also partly explained by photo-inhibition of CH₄ oxidizers in the illuminated zone. Sunlight appeared as an overlooked but important factor determining the CH₄ dynamics in surface waters, directly affecting its production by photoautotrophs and consumption by methanotrophs.

1. Introduction

25 Emissions from inland waters are an important component of the global CH₄ budget (Bastviken et al. 2011), in particular from tropical latitudes (Borges et al. 2015). While progress has been made in evaluating the CH₄ emission rates, much less attention has been given to the underlying microbial production (methanogenesis) and loss (methane oxidation) processes. It is generally assumed that CH₄ in lakes originates from the degradation of organic matter in anoxic sediments. Because most methanogens are considered to be strict anaerobes and net vertical diffusion of CH₄ from anoxic bottom waters is often negligible (Bastviken
30 et al. 2003), physical processes of CH₄ transport from shallow sediments are usually invoked to explain patterns of local CH₄ concentration maximum in surface waters (Encinas-Fernandez et al. 2016, Peeters et al. 2019, Martinez-Cruz et al. 2020). Indeed, CH₄-rich pore water is regularly released from littoral sediment into the water column during resuspension events associated with surface waves (Hofmann et al. 2010).

The view that CH₄ is formed under strictly anaerobic conditions has been challenged by several recent studies which proposed
35 that acetoclastic methanogens directly attached to phytoplankton cells are involved in epilimnetic CH₄ production (Grossart et al. 2011, Bogard et al. 2014), and are responsible of distinct near-surface peaks of CH₄ concentration in certain thermally stratified, well-oxygenated waterbodies (Tang et al. 2016). It has also been showed that Cyanobacteria (Bizic et al. 2020) and widespread marine phytoplankton (Klitzsch et al. 2019) are able to release substantial amount of CH₄ during a culture study, and this CH₄ production mechanism might be linked to photosynthesis. From a model-based approach, epilimnetic CH₄
40 production was shown to sustain most of the CH₄ oxidation in 14 Canadian lakes (DelSontro et al. 2018), and would even



represent up to 90% of the CH₄ emitted from a temperate lake (Donis et al. 2017). Further, empirical models based on data gathered in boreal and temperate lakes predict that the contribution of oxic CH₄ increases with lake size (Gunthel et al. 2019) and should represent the majority of CH₄ emissions in lakes larger than 1 km². Still, aerobic CH₄ production has so far only been documented in temperate and boreal lakes so that such predictive models could not directly apply to tropical lakes which
45 differ from their temperate counterparts in some fundamental characteristics, such as year-round elevated water temperature. Among others, primary production, methanogenic and methanotrophic activities, and cyanobacterial dominance are potentially much higher in tropical lakes due to favorable temperature (Lewis 1987, Kosten et al. 2012). It has also been shown that CH₄ emissions are positively related to temperature at the ecosystem scale (Yvon-Durocher et al. 2014)

Here, we tested the hypothesis that phytoplankton metabolism could fuel CH₄ production in well-oxygenated waters in five
50 contrasting tropical lakes in East Africa covering a wide range of size, depth, and productivity (L. Edward, L. George, L. Katinda, L. Nyamusingere and L. Kyambura). Phytoplankton activity could provide diverse substrates required for CH₄ production mediated by methanogenic Archaea, or alternatively CH₄ could be directly released by phytoplankton cells. Additionally, the significance of epilimnetic CH₄ production at the scale of the aquatic ecosystem was assessed by quantifying CH₄ release from sediments, CH₄ production and oxidation rates in the water column, and CH₄ diffusive and ebullitive
55 emissions to the atmosphere.

2. Material and methods

2.1. Site description

The sampled lakes cover a wide range of size (<1 to 2300 km²), maximum depth (3-117 m), mixing regimes, phytoplankton biomass and primary productivity (Table S1). Oligotrophic L. Kyamwinda (-0.18054°N, 30.14625°E) and eutrophic L. Katinda
60 (-0.21803°N, 30.10702°E) are stratified, small but deep tropical lakes located in Western Uganda. Neighboring L. Nyamusingere (-0.284364°N, 30.037635°E) is a small but shallow and polymictic eutrophic lake. L. George is a larger (250 km²), hypereutrophic, shallow lake located at the equator (-0.02273°N, 30.19724°E). A single outlet (Kazinga Channel) flows from L. George to the neighboring Lake Edward (-0.28971°N, 29.73327°E), a holomictic, mesotrophic large lake (2325 km²). Water samples from pelagic stations of L. Katinda, L. George (2km offshore) and L. Edward (15 km offshore) were collected
65 in April 2017 (rainy season) and January 2018 (dry season). Pelagic sites of L. Kyamwinda and L. Nyamusingere were sampled only once, in April 2017 and January 2018, respectively.

2.2. Environmental setting of the study sites

Conductivity, temperature and dissolved oxygen concentration measurements were performed with a Yellow Spring Instrument EXO II multiparametric probe. Samples for particulate organic carbon (POC) concentration were collected on glass
70 fiber filters (0.7 μm nominal pore size) and analyzed with an elemental analyzer coupled to an isotope ratio mass spectrometer (EA-IRMS) (Morana et al. 2015). Pigment concentrations were determined by high performance liquid chromatography (Descy et al. 2016) after filtration of water samples through glass fiber filters (0.7 μm nominal pore size).

Water samples for determination of dissolved CH₄ concentration were transferred with tubing from the Niskin bottle to 60 ml borosilicate serum bottles that were poisoned with 200μL of a saturated solution of HgCl₂, closed with a butyl stopper
75 and sealed with an aluminum cap. The concentrations of dissolved CH₄ was measured with the headspace equilibration technique (20 ml headspace) using a gas chromatograph with flame ionization detection (GC-FID, SRI8610C).

Samples for δ¹³C-CH₄ determination were collected in 60 ml serum bottles following the same procedure than samples for CH₄ concentration determination. In the laboratory, δ¹³C-CH₄ was measured as described in Morana et al. (2015). Briefly, a 20ml helium headspace was created in the serum bottles, then samples were vigorously shaken and left to equilibrate
80 overnight. The sample gas was flushed out through a double-hole needle and purified of non-CH₄ volatile organic compounds



in a liquid N₂ trap, CO₂ and H₂O were removed with a soda lime and a magnesium perchlorate traps, and the CH₄ was converted to CO₂ in an online combustion column similar to that in an elemental analyzer (EA). The resulting CO₂ was subsequently preconcentrated in a custom-built cryo-focussing device by immersion of a stainless-steel loop in liquid N₂, passed through a micro-packed GC column (HayeSep Q 2 m, 0.75mm ID; Restek), and finally measured on a Thermo Scientific Delta V
85 Advantage isotope ratio mass spectrometer (IRMS). CO₂ produced from certified reference standards for δ¹³C analysis (IAEA-CO1 and LSVEC) were used to calibrate δ¹³C-CH₄ data. Reproducibility of measurement estimated based on duplicate injection of a selection of samples was typically better than 0.5 ‰, or better than 0.2‰ when estimated based on multiple injection of standard gas.

2.3. Diffusive CH₄ flux calculation

90 Surface CH₄ concentrations were used to compute the diffusive air-water CH₄ fluxes (FCH₄) according to eq. (1):

$$FCH_4 = k \times \Delta CH_4 \quad (1)$$

Where k is the gas transfer velocity of CH₄ computed from wind speed (Cole & Caraco 1998) and the Schmidt number
95 of CH₄ in freshwater (Wanninkhof 1992), and ΔCH₄ is the air-water gradient. Wind speed data were acquired with a Davis Instruments meteorological station located in Mweya peninsula (0.11°S 29.53°E).

2.4. CH₄ ebullition flux

CH₄ ebullition flux was investigated in In L. Edward, George, and Nyamusingere only. Bubble traps made with an inverted funnel (24 cm diameter) connected to a 60 ml syringe were deployed for a period between 24 h and 48 h at 0.5 m
100 below the water surface (4 replicates). Measurements were performed at sites with water depth of 20 m, 2.5 m and 3 m for L. Edward, George and Nyamusingere, respectively. After measuring the gas volume collected within the trap during the sampling period, the gas bubbles were transferred in a tightly closed 12 ml Exetainer vial (Labco) for subsequent analysis of their CH₄ concentration. Variability of the gas volume in the 4 replicates was less than 10%. We used the SiBu-GUI software (McGinnis et al. 2006, Greinert et al. 2009) to correct for gas exchange within the water column during the rise of bubbles and
105 thus obtained the CH₄ ebullition and CH₄ bubble dissolution fluxes. Calculations were made following several scenarios: two extreme bubble-size scenarios considering a release of many small (3 mm diameter) bubbles or fewer large (10 mm) bubbles, and an intermediate scenario of release of 6 mm diameter bubbles.

2.5. CH₄ flux across the sediment-water interface

CH₄ flux across the sediment-water interface was determined from short-term intact core incubations in L. Edward,
110 L. George and L. Nyamusingere only. CH₄ flux was quantified from the change of CH₄ concentration in overlying waters at 5 different time steps, every 2 hours. Briefly, in every lake, 2 sediment cores (6 cm wide; ~ 30cm sediment and 30cm of water) were collected taking care to avoid disturbance at the sediment-water interface. Cores were kept in the dark until back in the laboratory, typically 6h later. Overlying water was carefully removed and replaced by bottom lake water filtered through 0.2µm polycarbonate filters (GSWP, Millipore) in order to remove water column methanotrophs. It was then degassed with
115 helium during 20 minutes in order to remove background O₂ and CH₄, and gently returned in the core tubes, on top of the sediments. Core tubes were tightly closed with a thick rubber stopper equipped with two sampling valves. A magnetic stirrer placed ~ 10 cm above the sediments was allowed to rotate gently in order to homogenize the overlying water layer during the incubation. At each time step, 60 ml of overlying water was sampled by connecting a syringe to the first sampling valve while an equivalent volume of degassed water was allowed to flow through the second valve in order to avoid any pressure
120 disequilibrium. Subsamples of overlying water were transferred into a two 20 ml serum bottles filled without headspace and



poisoned with HgCl₂. Determination of the dissolved CH₄ concentration was performed with a GC-FID following the same procedure as described above.

2.6. Primary production and N₂ fixation

Primary production and N₂ fixation rates were determined from dual stable isotope photosynthesis-irradiance experiments using NaH¹³CO₃ (Eurisotop) and dissolved ¹⁵N₂ (Eurisotop) as tracers for incorporation of dissolved inorganic carbon (DIC) and N₂ into the biomass. The ¹⁵N₂ tracer was added dissolved in water (Mohr et al. 2010). Incident light intensity was measured by a LI-190SB quantum sensor during day time during the entire duration of the sampling campaign. At each station a sample of surface waters (500 ml) was spiked with the tracers (final ¹⁵N atom excess ~5%). Three subsamples were preserved with HgCl₂ in 12-mL Exetainers vials (Labco) for the determination of the exact initial ¹³C-DIC and ¹⁵N-N₂ enrichment. The rest of the sample was divided into nine 50-ml polycarbonate flasks, filled without headspace. Eight flasks were placed into a floating incubation device providing a range of light intensity (from 0 to 80% of natural light) using neutral density filter screen (Lee Filters). The last one was immediately amended with neutral formaldehyde (0.5% final concentration) and served as killed control sample. Samples were incubated *in situ* during 2 hours around mid-day just below the surface at lake surface temperature. After incubation, biological activity was stopped by adding neutral formaldehyde into the flasks, and the nine samples were filtered on pre-combusted GF/F filters when back in the lab. Glass fiber filters were decarbonated with HCl fumes overnight, dried, and their δ¹³C-POC and δ¹⁵N-PN values were determined with an EA-IRMS (Thermo FlashHT – delta V Advantage). For the measurement of the initial ¹⁵N₂ enrichment, a 2-ml helium headspace was created, and after 12h equilibration, a fraction of the headspace was injected into the above-mentioned EA-IRMS equipped with a Cu column warmed at 640°C and a CO₂ trap. Initial enrichment of ¹³C-DIC was also measured.

Photosynthetic (P_i) (Hama et al. 1983) and N₂ fixation (N₂fix_i) (Montoya et al. 1996) rates in individual bottles were calculated, and corrected for any abiotic tracer incorporation by subtraction of the killed control value. For each experiment, the maximum photosynthetic and N₂ fixation rates (P_{max}, N₂fix_{max}) and the irradiance at the onset of light saturation (I_{k,pp}, I_{k,N2fix}) were determined by fitting P_i and N₂fix_i to the light intensity gradient provided by the incubator (I_i) using the equation (eq. 2) for photosynthesis activity (Vollenweider 1965) and (eq. 3) for N₂ fixation (Mugidde et al. 2003).

145

$$P_i = 2P_{max} \left[\frac{I_i/2I_{k,pp}}{1 + (I_i/2I_{k,pp})^2} \right] \quad (2)$$

$$N_2fix_i = 2N_2fix_{max} \left[\frac{I_i/2I_{k,N2fix}}{1 + (I_i/2I_{k,N2fix})^2} \right] \quad (3)$$

150 2.7. Determination of CH₄ oxidation rates.

CH₄ oxidation rates in surface waters (1m depth) were determined from the decrease of CH₄ concentrations measured during short (typically < 24h) time course experiments. Samples for CH₄ oxidation rate measurement were collected in 60 mL glass serum bottles filled directly from the Niskin bottle with tubing, left to overflow, and immediately closed with butyl stoppers previously boiled in milli-Q water, and sealed with aluminum caps. The first bottle was then poisoned with a saturated solution of HgCl₂ (100 μl) injected through the butyl stopper with a polypropylene syringe and a steel needle and corresponded to the initial CH₄ concentration at the beginning of the incubation (T₀).

The remaining bottles were incubated in the dark, at *in situ* (~26°C) temperature during ~12h or ~24h except in L. George and Nyamusingere where the incubation was shorter (~6h). At 4 different times step one bottle was poisoned with 100 μL of HgCl₂ and stored in the dark until measurement of the CH₄ concentrations with the above-mentioned GC-FID. CH₄ oxidation rates were calculated as a linear regression of CH₄ concentrations over time (r² generally better than 0.80) during the course of the incubation.

160



2.8. Sunlight inhibitory effect on CH₄ oxidation

The influence of light intensity on methanotrophy was investigated in Lake Edward and Lake George by means of a stable isotope (¹³CH₄) labelling experiment. For each experiment, 12 serum bottles (60 mL) were filled with lake surface waters (1m) as described above. All bottles were spiked with 100 μL of a solution of dissolved ¹³CH₄ (50 μmol L⁻¹ final concentration, 99% enrichment) added in excess. Half of the bottles were amended with 3-(3,4-dichlorophenyl)-1,1-dimethylurea (DCMU, 0.5 mg L⁻¹) in order to inhibit photosynthesis (Bishop 1958) and investigate the hypothetical inhibitory effect of dissolved O₂ production by phytoplankton. Two bottles were poisoned immediately with pH-neutral formaldehyde (0.5% final concentration) and served as killed controls. The ten others were incubated during 24h at 26°C in a floating device providing 5 different light intensities (from 0 to 80% of natural light using neutral density filter screens (Lee Filters). For every bottle at the end of the incubation, one 12-mL vial (Labco Exetainer) was filled with the water sample and preserved with 50 μL HgCl₂. The rest of the sample (~50 mL) was filtered on a precombusted GF/F filter for subsequent δ¹³C-POC measurement.

δ¹³C-DIC and δ¹³C-POC were determined with an EA-IRMS as described above. The methanotrophic bacterial production, defined at the CH₄-derived ¹³C incorporation rates into the POC pool was calculated as in eq. (4) (Morana et al. 2015):

$$MBP = \frac{POC_t \times (\%^{13}CPOC_t / \%^{13}CPOC_i)}{t \times (\%^{13}CCH_4 / \%^{13}CPOC_i)} \quad (4)$$

Where POC_t is the concentration of POC after incubation, %¹³C-POC_t and %¹³C-POC_i are the final and initial percentage of ¹³C in the POC, t is the incubation time and %¹³C-CH₄ is the percentage of ¹³C in CH₄ after the inoculation of the bottles with the tracer. Similarly, the methanotrophic bacterial respiration rates, defined as the CH₄-derived ¹³C incorporation rates into the DIC pool, were calculated as in eq. (5):

$$MBR = \frac{DIC_t \times (\%^{13}CDIC_t / \%^{13}CDIC_i)}{t \times (\%^{13}CCH_4 / \%^{13}CDIC_i)} \quad (5)$$

Where DIC_t is the concentration of DIC after the incubation, %¹³C-DIC_t and %¹³C-DIC_i are the final and initial percentage of ¹³C in DIC and %¹³C-CH₄ is the percentage of ¹³C in CH₄ after the inoculation of the bottles with the tracer.

Potential CH₄ oxidation rates (MOX) were calculated as the sum of MBP and MBR rates. The fraction (%) of MOX inhibited by light was calculated at every light intensity as (eq.6):

$$MOX_{inhibition}(\%) = (1 - MOX_i / MOX_{dark}) \times 100 \quad (6)$$

Where MOX_i is the potential CH₄ oxidation for a given light treatment and MOX_{dark} is the potential CH₄ oxidation in the dark.

2.9. Determination of pelagic CH₄ production rates.

Time course ¹³C tracer experiments were carried out in well oxygenated surface waters at every sampling site. Measurement of the isotopic enrichment of the CH₄ during this experiment allowed to estimate production rates of CH₄ issued from 3 different precursors: ¹³C-DIC (NaH¹³CO₃), ¹³C_(1,2)-acetate and ¹³C_{methyl}-methionine. Serum bottles (60 ml) were spiked with 1 ml of ¹³C tracer solution, or with an equivalent volume of distilled water for the control treatment. NaH¹³CO₃ was added in the bottles at a tracer level (less than 5% of ambient HCO₃⁻ concentration) while ¹³C_(1,2)-acetate and ¹³C_{methyl}-methionine were added largely in excess (>99% of ambient concentration). Therefore, we assume the CH₄ production rates measured from ¹³C-DIC could be representative of in-situ rates, but the production rates measured from ¹³C-acetate and ¹³C-methionine should



instead be viewed as potential rates. The exact amount of ^{13}C -DIC added in the bottles was determined filling a borosilicate 12 ml exetainer vials preserved and analysed for $\delta^{13}\text{C}$ -DIC as described above.

205 The control bottles and the bottles amended with the different ^{13}C tracer were incubated under constant temperature conditions (26°C) following three different treatments : (1) one third were incubated under constant light (PAR of $\sim 200 \mu\text{mol photon m}^{-2} \text{s}^{-1}$), (2) another third were incubated under the same light intensities conditions but were first amended with DCMU (0.5 mg L^{-1} ; final concentration), an inhibitor of photosynthesis, (3) and the last third were incubated in the dark.

210 At each time step (typically every 6-12h, 5-time steps), the biological activity was stopped by adding $100 \mu\text{L}$ of a saturation solution of HgCl_2 . Bottles were kept in the dark until CH_4 concentration measurement and $\delta^{13}\text{C}$ - CH_4 determination as described above.

The term $\text{CH}_4_{\text{prod}}$ ($\text{nmol L}^{-1} \text{h}^{-1}$) defined as the amount of CH_4 produced from a specific tracer during a time interval t (h), was calculated following this equation (eq. 7) derived from Hama et al. (1983):

$$\text{CH}_4_{\text{prod}} = \frac{\text{CH}_{4,t} \times (\%^{13}\text{CCH}_{4,t} / \%^{13}\text{CCH}_{4,i})}{t \times (\%^{13}\text{Ctracer} / \%^{13}\text{CCH}_{4,i})} \quad (7)$$

215

Where $\text{CH}_{4,t}$ and $\%^{13}\text{CCH}_{4,t}$, represent the CH_4 concentration (nmol L^{-1}) and the $\%^{13}\text{C}$ atom of the CH_4 pool at a given time step, respectively. $\%^{13}\text{CCH}_{4,i}$ represent the $\%^{13}\text{C}$ atom of the pool of CH_4 at the beginning of the experiment. $\%^{13}\text{Ctracer}$ represent the $\%^{13}\text{C}$ atom of the isotopically enriched pool of the precursor molecule tested (NaHCO_3 , methionine or acetate, depending of the treatment). $\%^{13}\text{C}$ -tracer was assumed constant during the full course of the incubation given the 220 high concentration of ambient DIC in the sampled lakes ($\sim 2 \text{ mmol L}^{-1}$ in L. George, $> 6 \text{ mmol L}^{-1}$ in the other lakes) and that acetate and methionine were spiked in large excess ($>99\%$).

2.10. DNA extraction

Surface water sample for DNA analysis (between 1 L and 0.15 L, depending on the biomass) were first filtered through $5.0 \mu\text{m}$ pore size polycarbonate filters (Millipore). The eluent was then subsequently filtered through $0.2 \mu\text{m}$ pore size 225 polycarbonate filters (Millipore) to retain free living prokaryotes. Filters were stored frozen (-20°C) immersed in a lysis buffer until processing in the laboratory. Total DNA was extracted from the $0.2 \mu\text{m}$ and $5.0 \mu\text{m}$ 47 mm filters using DNeasy PowerWater kit (Qiagen) following the manufacturer's instructions. Quality and quantity of the extracted DNA were estimated using the NanoDrop ND-1000 spectrophotometer (ThermoFisher) and the Qubit 3.0 fluorometer (Life technology). Extracted DNA was stored at -20°C until further use.

230 2.11. Quantification of *mcrA* via qPCR

Quantification of *mcrA* gene copies was performed by quantitative PCR (qPCR) on the total extracted DNA. The used primer pair consisted of forward primer *qmcrA-F* 5'-TTCGGTGGATCDCARAGRGC-3' and *qmcrA-R* 5'-GBARGTCGAWCCGTAGAATCC-3' (Denman et al. 2007). The reaction mixture contained $3 \mu\text{L}$ of total community DNA extract, $7.5 \mu\text{L}$ Absolute qPCR SYBR Green Mix (ThermoFisher, Cat. AB1158B), $0.3 \mu\text{L}$ of $10 \mu\text{M}$ forward primer 235 *mcrF*, $0.3 \mu\text{L}$ of $10 \mu\text{M}$ reverse primer *mcrR*, $1.5 \mu\text{L}$ of a 1% w/v Bovine Serum Albumin solution (Amersham Bioscience) and $2.4 \mu\text{L}$ of Nuclease/DNA-free water. The qPCR was performed in a Rotorgene 3000 (Corbett Research) using the following conditions: 95°C (15 min) followed by 40 cycles of 20 s at 95°C , 20 s at 58°C , 20 s at 72°C and a final extension step of 5 s at 80°C . Standard curves were prepared from serial dilutions of a prequantified *mcrA* PCR fragment amplified using primers *mcrF* and *mcrR* from a plasmid extract carrying the complete *mcrA* gene using concentrations ranging from 240 1×10^2 to 1×10^8 copies μL^{-1} . Samples were analyzed in triplicates.

2.12. 16S rRNA gene amplicon sequencing



Sequencing of the 16S rRNA gene was done on the total extracted DNA to assess community composition. 16S rRNA gene sequencing was done with the Illumina MiSeq v3 Chemistry following the “16S Metagenomic Sequencing Library Preparation” protocol with the following universal 16S rRNA gene primers targeting the V4 region, forward UniF/A519F-(S-
245 D-Arch-0519-a-S-15) 5'-CAGCMGCCGCGGTAA-3' and reverse UniR/802R-(S-D-Bact-0785-b-A-18) 5'-TACNVGGTATCTAATCC-3' (Klindworth et al. 2013). Sequenced read quality was checked using FastQC v0.11 (<https://www.bioinformatics.babraham.ac.uk/projects/fastqc/>). Short reads were trimmed to 250 bp with FastX Toolkit v0.0.13 (http://hannonlab.cshl.edu/fastx_toolkit/) in order to remove trailing Ns and low quality bases. Operational Taxonomical Units (OTU) for each analyzed sample were obtained from the quality trimmed reads using mothur v1.39.5 (Kozich et al. 2013) and
250 following the online MiSeq SOP (https://mothur.org/wiki/MiSeq_SOP - accessed April 2018) using the Silva v128 16S rRNA database with the following parameters: *maxambig* = 0 bp; *maxlength* = 300 bp; *maxhomop* = 8; and classify OTUs to 97% identity. Generated OTU table was used to calculate relative abundances of each OTU per sample.

3. Results and discussion

3.1. Patterns of phytoplankton biomass and dissolved CH₄

255 The sampled lakes cover a wide range of size (<1 to 2300 km²), maximum depth (3-117 m), mixing regimes, phytoplankton biomass and primary productivity (Table S1, Fig. S1). Phytoplankton biomass (Chlorophyll-a from 3.6 μg L⁻¹ to 190.2 μg L⁻¹) was dominated by Cyanobacteria (>95%) in the most productive lakes, while Diatoms (<20%) and Chrysophytes (<40%) also contributed in the less productive ones (Fig. S2). Maximum potential photosynthetic activity (*P_{max}*) varied from 1.5 μmol C L⁻¹ h⁻¹ in L. Edward to 199.0 μmol C L⁻¹ h⁻¹ in L. George and was linearly related to chlorophyll a concentration. Light-dependent N₂ fixation was detected in every lake with the exception of L. Kyamwinda. No significant N₂
260 fixation rates were measured in the dark. Maximum potential N₂ fixation rates (*N₂fix_{max}*) ranged between 1 nmol L⁻¹ h⁻¹ and 128 nmol L⁻¹ h⁻¹ and were positively related to *P_{max}* (Fig. S1).

We detected and quantified the abundance of the archaeal alpha subunit of methyl-coenzyme M reductase gene (*mcrA*), a proxy for methanogens, in the surface waters of each lake. *mcrA* gene copy abundance (*mcrA* copy ng DNA⁻¹) ranged
265 between 319 ± 41 (L. Edward) and 7537 ± 476 (L. Katinda) in the fraction of seston < 5 μm, and between 541 ± 19 (L. Edward) and 7968 ± 167 (L. Katinda) in the fraction of seston > 5 μm (Fig. S3). Illumina 16S rRNA gene amplicon sequencing indicated that methanogens accounted for a small fraction of the prokaryotic community in the surface waters of L. Edward (0.01 %), L. Kyamwinda (0.03 %) and L. Nyamusingere (0.08 %). They represented a substantially higher fraction of the community in L. Katinda (0.38%) and L. George (0.57 %) (Fig. S4). In all lakes, hydrogenotrophic (*Methanomicrobiales* and
270 *Methanobacteriales*) were always more abundant than acetoclastic (*Methanosarcinales*) microorganisms, representing at least 65% of the methanogens (up to 95% in L. Katinda, Fig. S4).

Surface waters were super-saturated in CH₄ in all lakes, with surface concentrations (at 1 m) ranging between 78 and 652 nmol L⁻¹ (atmospheric equilibrium ~ 2 nmol L⁻¹). Vertical patterns of CH₄ and stable carbon isotope composition of CH₄ (δ¹³C-CH₄) were variable among the different lakes. In L. Kyamwinda and Katinda, higher CH₄ concentrations and lower δ¹³C-
275 CH₄ values were observed in the well-oxygenated epilimnion compared to the metalimnion showing a source of relatively ¹³C-depleted CH₄ to the epilimnetic CH₄ pool (Fig. 1). The CH₄ concentrations and δ¹³C-CH₄ were homogeneous in the water column of L. Edward that is much larger than the other studied lakes (2300 km², Table S1) and characterized by a higher wind exposure and a substantially weaker thermal stratification (Fig. 1). However, a clear horizontal gradient in CH₄ concentration and δ¹³C-CH₄ occurred between the littoral and pelagic zones (Fig. S5). Vertical gradients were also observed at much smaller
280 scale in the near sub-surface (top 0.3 m) in the shallow and entirely well oxygenated L. George and L. Nyamusingere (Fig. 2). In both lakes CH₄ concentrations were relatively modest in the hypolimnion (< 50 nmol L⁻¹) but increased abruptly in the thermal gradient (0.3 m interval) to reach a surface maximum > 240 nmol L⁻¹ (Fig. 2). δ¹³C-CH₄ mirrored this pattern with



significantly lower values in surface than at the bottom of the water column indicating that a source of relatively ^{13}C -depleted CH_4 contributed to the higher epilimnetic CH_4 .

285 3.2. Occurrence of microbial CH_4 production in surface waters

Despite the prevalence of oxic conditions, ^{13}C -labelling experiments revealed that CH_4 was produced in surface waters of each lake with the exception of L. Kyamwinda (Fig. 3). The kinetic of incorporation of $\text{NaH}^{13}\text{CO}_3$ into the CH_4 pool revealed that a substantially higher amount of CH_4 was produced from dissolved inorganic carbon (DIC) in illuminated waters, and this mechanism of CH_4 formation appears to be related to photosynthesis, as none or only modest quantities of CH_4 were
290 produced from ^{13}C -labelled DIC under darkness or when photosynthesis was inhibited by DCMU (Figs. 3a and S6). Furthermore, CH_4 production from DIC appeared strongly correlated ($r^2 = 0.91$) to the photosynthetic activity (Fig. 4a) and N_2 fixation rates (Fig 4b), supporting the view that CH_4 formation in oxic waters was directly linked to phytoplankton metabolism (Bizic et al. 2020).

Aside from DIC, an appreciable amount of CH_4 was generated in all lakes from the sulfur bonded methyl group of
295 methionine when bottles were incubated under light, irrespective of the addition of DCMU (Fig. 3b and S6), that were approximately 4 times higher than in the dark. In addition, a positive relationship between CH_4 production from methionine in the light and the photosynthetic activity was found (Fig. 4c).

^{13}C -labelled acetate, the substrate of acetoclastic methanogenesis, supported the production of CH_4 in all lakes with the exception of L. Kyamwinda, but at much lower rates compared to light-dependent CH_4 production from DIC (50 times
300 lower, $n=7$) or methionine (10 times lower, $n=4$) (Fig. 3c and S6). $\delta^{13}\text{C}$ analysis of the DIC in the bottles spiked with ^{13}C -labelled acetate showed that the acetate was mineralized at rates of 5-6 orders of magnitude higher than acetoclastic methanogenesis so that added acetate appeared to be used almost exclusively by heterotrophic micro-organisms other than methanogens. Pattern of acetate-derived production of CH_4 were similar in light and dark treatments (Figs. 3c and S6) and this mode of CH_4 production appeared unrelated to phytoplankton activity (Fig. 4d).

305 3.3. Mechanisms of epilimnetic CH_4 production

Only a minimal fraction of the CH_4 produced under aerobic conditions originated from acetate in contrast with several earlier studies (Bogard et al. 2014, Donis et al. 2017) which proposed, based on the apparent fractionation factor of $\delta^{13}\text{C}\text{-CH}_4$, that acetoclastic methanogenesis linked to phytoplankton production of organic matter would be the dominant biochemical pathway of pelagic CH_4 production in oxic freshwaters. Instead, our results suggest that epilimnetic CH_4 production in well-
310 oxygenated conditions was related to DIC fixation by photosynthesis (Fig. 3), and correlated to primary production (Fig. 4a) and N_2 fixation (Fig 4b). When normalized to POC concentrations, the average DIC-derived CH_4 production rates (0.08 ± 0.05 $\text{nmol mmol}_{\text{POC}}^{-1} \text{h}^{-1}$ $n = 7$) was remarkably similar to the CH_4 production rates recently reported in Cyanobacteria cultures (0.04 ± 0.02 $\text{nmol mmol}_{\text{POC}}^{-1} \text{h}^{-1}$) grown at 30°C , among which the freshwater *Microcystis aeruginosa* (Bizic et al. 2020), the dominant Cyanobacterium species in the tropical lakes investigated in our study (see Fig S2). These CH_4 production rates are
315 2 orders of magnitude higher than rates reported in an axenic culture of the eukaryote *Emiliana huxleyi* (0.19 ± 0.07 $\text{pmol mmol}_{\text{POC}}^{-1} \text{d}^{-1}$) (Lenhart et al. 2016), but they are 4 orders of magnitude lower than typical anoxic CH_4 production rates by methanogenic Archaea (Mountford & Asher 1979). Although it seems improbable that ^{13}C -DIC acted as a direct precursor molecule for the CH_4 released by phytoplankton (Lenhart et al. 2016, Klintzsch et al. 2019) ^{13}C -DIC could have been taken up by phytoplankton cells and then used as a C source for the synthesis of many different organic molecules that may serve as the
320 actual CH_4 precursors. Indeed, healthy phytoplankton cells actively release a variety of low molecular weight molecules which are generally highly labile and rapidly consumed (Baines & Pace 1991, Morana et al. 2014). Phytoplankton metabolism could have fuelled CH_4 production pathways, at least partially, excreting substrates involved in CH_4 production via biochemical



processes such as demethylation of a variety of organic molecules like methionine, one of the S-bonded methylated amino acids (Lenhart et al. 2016), trimethylamine (Bizic et al 2018), or methylphosphonate (Yao et al. 2016).

325 While the source of methylphosphonate in freshwaters is obscure and its actual natural abundance remains to be determined, dissolved free amino acids would represent up to 4% of the DOC produced by phytoplankton and are rapidly consumed by heterotrophic bacteria (Sarmiento et al. 2013). Our incubations indeed demonstrated that the methyl group of methionine was a potential precursor of CH₄ in all lakes investigated, in line with recent findings showing that *Emiliana huxleyi* could act as a direct source of CH₄ in oxic conditions using methionine as precursor, without involvement of any other
330 micro-organisms (Lenhart et al. 2016). We found that CH₄ production from methionine was clearly stimulated under light, even when photosynthetic activity was inhibited by DCMU, while little CH₄ from methionine was produced in darkness (Fig. 3b). DCMU notably prevents reduction of plastoquinone at photosystem II and generates singlet oxygen (Petrillo et al. 2014). The mechanism of CH₄ production from methionine is still unclear, but its residue in proteins is particularly sensitive to oxidation to methionine sulfoxide by radical oxygen species (ROS) (Levine et al. 1996) so that methionine would act as an
335 effective ROS scavenger and play important protective roles under photooxidative stress conditions, as shown in vascular plants (Bruhn et al. 2012). The side chain of methionine sulfoxide is identical to dimethyl sulfoxide which is known to react with hydroxyl radicals (OH) to form CH₄ (Repine et al. 1979). Besides its photoprotective role for phytoplankton, methionine could also be catabolized by a wide variety of microorganisms to methanethiol, which could in turn be transformed to CH₄ as shown in Arctic Ocean surface waters (Damm et al. 2010). Nevertheless, occurrence of this latter mechanism in the tropical
340 lakes investigated seems unlikely as this mode of CH₄ production would be expected to be insensitive to light irradiance and no CH₄ was produced from methionine in the dark during the incubations.

3.4. Relevance of epilimnetic CH₄ production compared to CH₄ loss terms at ecosystem scale

Net CH₄ oxidation was detected in all 5 investigated lakes ranging from 11 to 5212 nmol L⁻¹ d⁻¹ (Fig. 5), and was by far the largest loss term of dissolved CH₄ at ecosystem scale (8 to 46 times higher than the diffusive emission to the
345 atmosphere). Surface water CH₄ turnover times were particularly short in the shallow and eutrophic L. George (2h) and L. Nyamusingere (3h) and slightly longer in the deeper and less productive L. Katinda (11h), L. Kyamwinda (77h) and L. Edward (100h). In all studied lakes, pelagic CH₄ production rates measured during the stable isotope tracer experiments represented between 0.1% and 8.5% of net CH₄ oxidation rates, regardless of the CH₄ precursors tested.

All of the major sources and sinks of CH₄ at ecosystem scale were experimentally determined offshore in three lakes
350 (L. Edward at 20 m depth, George and Nyamusingere) (Fig. 6). In these three lakes, surface CH₄ production rates from the diverse precursors molecules investigated were modest relative to the diffusive CH₄ efflux to the atmosphere (0.4 – 20.0 %) and microbial CH₄ oxidation (0.1 – 13.2 %). In opposition, the combined CH₄ bubble dissolution flux and diffusive benthic CH₄ flux were several orders of magnitude higher than CH₄ production in surface waters, and met the CH₄ loss terms (emission and oxidation) (Fig. 6). These results gathered in tropical lakes of various size (from 0.44 to 2300 km²) and depth are in sharp
355 contrast with the estimation of an empirical model (Gunthel et al. 2019) which proposed that mechanisms of oxic CH₄ production represents the majority of CH₄ emissions in lakes larger than 1 km². This discrepancy highlights the need to consider the unique limnological characteristics of a vast region of the world that harbours 16% of the total surface of lakes (Lehner & Doll 2004). One of the most distinctive features of tropical aquatic environment is the persistent elevated water temperature in the hypolimnion and at the water-sediment interface which favours methanogenic activity in sediment and decreases CH₄
360 solubility, enhancing bubbles formation.

3.5. Origin of ¹³C depleted CH₄ in surface waters

Epilimnetic CH₄ production was a marginal flux at ecosystem scale and could not explain alone the accumulation of ¹³C-depleted CH₄ in the epilimnion of most of the lakes of our dataset (Figs. 1, 2), for which we propose two other alternative



mechanisms: dissolution of arising CH₄ bubbles in the epilimnion combined with inhibition by light of CH₄ oxidation. The
365 partial dissolution of the CH₄ bubbles as they rise in the epilimnion should allow a rapid transport of ¹³C-depleted CH₄ from
the sediment, bypassing the hotspot of CH₄ oxidation at the sediment-water interface and representing an alternative source of
¹³C-depleted CH₄ in water column. The shallower L. George and L. Nyamusingere were notably characterized by sharp thermal
density gradients (Fig. 2) and extreme phytoplankton biomass largely dominated by *Microcystis aeruginosa* (Chlorophyll a up
to 190 µg L⁻¹). *Microcystis aeruginosa* cells form large aggregates (>1 mm) embedded in a matrix of extracellular polymeric
370 substance that might act as a barrier to trap small CH₄ bubbles arising from the sediment (Fig S7). Dissolution of CH₄ bubbles
could be enhanced at the very near surface due to the entrapments of bubbles at the air-water interface by abundant surface
organic films that delay the bubble “burst”. The presence of a sharp sub-surface temperature gradient would further enhance
CH₄ accumulation during day-time near the air-water interface (by blocking vertical redistribution of CH₄ by mixing). We
hypothesize that this process could be widespread in shallow tropical lakes which are characterized by high productivity and
375 are susceptible to be simultaneous large benthic CH₄ sources.

The influence of light on methanotrophy was investigated in the deep L. Edward, and shallow L. George and L.
Nyamusingere, revealing that CH₄ oxidation rates decreased dramatically with increasing light intensity (Fig. 5). For instance,
when exposed to full sunlight intensity, methanotrophs consumed only 42% (L. Edward), 54% (L. Nyamusingere) or 74% (L.
George) of the CH₄ they were able to oxidize in the dark. The magnitude of this light-induced inhibition decreased substantially
380 with decreasing sunlight intensities, as shown elsewhere (Murase & Sugimoto 2005). The physiological mechanism of
photoinhibition of CH₄ oxidation could be related to the fact that the copper-containing methane monooxygenase enzyme and
structurally close to the ammonia monooxygenase enzyme, and might be inactivated by ROS produced during photooxidative
stress, as shown for ammonium oxidizers (French et al. 2012, Tolar et al. 2016). Altogether, our results emphasize the role of
sunlight irradiance as an important, but frequently overlooked, environmental factor driving the CH₄ dynamics in lake surface
385 waters, and possibly contributing to the occurrence of ¹³C depleted CH₄ in surface waters.

4. Supplement

Supplementary figures are available on-line on the *Biogeosciences* website.

5. Data availability

All data included in this study are available upon request by contacting the corresponding author.

390 6. Author contributions

This study was designed by C. Morana, A.V. Borges & S. Bouillon. All authors participated to samples collection, data
acquisition and analysis, and to the drafting of the manuscript. All authors approved the final version of the manuscript.

7. Competing interests

The authors declare that they have no conflict of interest.

395 8. Acknowledgments

We are grateful to Marc-Vincent Commarieu and Dries Grauwels for their help in the lab and during the field sampling. We
also thank the Uganda Wildlife Agency for research permission in the Queen Elizabeth National Park (Uganda), the staff of
the Tembo Canteen for the use of their incubation room and the crew of the Katwe Marine Research Vessel for their help
during the L. Edward sampling. This work was funded by the Belgian Federal Science Policy Office (BELSPO, HIPE project,
400 BR/154/A1/HIPE) and by the Fonds Wetenschappelijk Onderzoek (FWO-Vlaanderen, Belgium) with travel grants awarded
to CM and SB. AVB is a research director at the Fond National de la Recherche Scientifique (FNRS, Belgium).

9. References



- Bastviken, D., Ejlertsson, J., Sundh, I., & Tranvik, L.: Methane as a source of carbon and energy for lake pelagic food webs. *Ecology*, 84(4), 969-981, 2003
- 405 Bastviken, D., Tranvik, L. J., Downing, J. A., Crill, P. M., & Enrich-Prast, A.: Freshwater methane emissions offset the continental carbon sink, *Science*, 331(6013), 50-50, 2011
- Baines, S. B., & Pace, M. L.: The production of dissolved organic matter by phytoplankton and its importance to bacteria: patterns across marine and freshwater systems. *Limnology and Oceanography*, 36(6), 1078-1090, doi: 10.4319/lo.1991.36.6.1078, 1991
- 410 Bishop, N. I.: The influence of the herbicide, DCMU, on the oxygen-evolving system of photosynthesis. *Biochimica et biophysica acta*, 27(1), 205-206, doi: 10.1016/0006-3002(58)90313-5, 1958
- Bižić, M., Ionescu, D., Günthel, M., Tang, K. W., & Grossart, H. P.: Oxidic Methane Cycling: New Evidence for Methane Formation in Oxidic Lake Water. *Biogenesis of Hydrocarbons*, 1-22, 2018
- Bižić, M., Klintzsch, T., Ionescu, D., Hindiyyeh, M. Y., Günthel, M., Muro-Pastor, A. M., Eckert, W., Ulrich, T., & 415 Grossart, H. P.: Aquatic and terrestrial cyanobacteria produce methane. *Science advances*, 6(3), eaax5343, doi: 10.1126/sciadv.aax5343, 2020
- Bogard, M. J., Del Giorgio, P. A., Boutet, L., Chaves, M. C. G., Prairie, Y. T., Merante, A., & Derry, A. M.: Oxidic water column methanogenesis as a major component of aquatic CH₄ fluxes. *Nature communications*, 5, 5350, doi: 10.1038/ncomms6350, 2014
- 420 Borges, A. V., Darchambeau, F., Teodoru, C. R., Marwick, T. R., Tamoo, F., Geeraert, N., Morana, C., Okuku, E., & Bouillon, S.: Globally significant greenhouse-gas emissions from African inland waters. *Nature Geoscience*, 8(8), 637-642, 2015
- Bruhn, D., Möller, I. M., Mikkelsen, T. N., & Ambus, P.: Terrestrial plant methane production and emission. *Physiologia plantarum*, 144(3), 201-209, doi: 10.1111/j.1399-3054.2011.01551, 2012
- 425 Cole, J. J., & Caraco, N. F.: Atmospheric exchange of carbon dioxide in a low-wind oligotrophic lake measured by the addition of SF₆. *Limnology and Oceanography*, 43(4), 647-656, doi: 10.4319/lo.1998.43.4.0647, 1998
- Damm, E., Helmke, E., Thoms, S., Schauer, U., Nöthig, E., Bakker, K., & Kiene, R. P.: Methane production in aerobic oligotrophic surface water in the central Arctic Ocean. *Biogeosciences*, 7(3), 1099-1108, doi: 10.5194/bg-7-1099-2010, 2010
- DelSontro, T., del Giorgio, P. A., & Prairie, Y. T.: No longer a paradox: the interaction between physical transport 430 and biological processes explains the spatial distribution of surface water methane within and across lakes. *Ecosystems*, 21(6), 1073-1087, doi: 10.1007/s10021-017-0205-1, 2018
- Denman, S. E., Tomkins, N. W., & McSweeney, C. S.: Quantitation and diversity analysis of ruminal methanogenic populations in response to the antimethanogenic compound bromochloromethane. *FEMS microbiology ecology*, 62(3), 313-322, doi: 10.1111/j.1574-6941.2007.00394.x, 2007
- 435 Descy, J. P., Darchambeau, F., Lambert, T., Stoyneva-Gaertner, M. P., Bouillon, S., & Borges, A. V.: Phytoplankton dynamics in the Congo River. *Freshwater Biology*, 62(1), 87-101, doi: 10.1111/fwb.1285, 2017
- Donis, D., Flury, S., Stöckli, A., Spangenberg, J. E., Vachon, D., & McGinnis, D. F. (2017). Full-scale evaluation of methane production under oxidic conditions in a mesotrophic lake. *Nature communications*, 8(1), 1661, doi: 10.1038/s41467-017-01648-4, 2017
- 440 Fernández, J. E., Peeters, F., & Hofmann, H.: On the methane paradox: Transport from shallow water zones rather than in situ methanogenesis is the major source of CH₄ in the open surface water of lakes. *Journal of Geophysical Research: Biogeosciences*, 121(10), 2717-2726, doi: 10.1002/2016JG003586, 2016
- French, E., Kozłowski, J. A., Mukherjee, M., Bullerjahn, G., & Bollmann, A.: Ecophysiological characterization of ammonia-oxidizing archaea and bacteria from freshwater. *Applied and Environmental Microbiology*, 78(16), 5773-5780, doi: 445 10.1128/aem.00432-12, 2012



- Greinert, J. and McGinnis, D.F.: Single Bubble Dissolution Model: The Graphical User Interface SiBu-GUI. *Environmental Modelling & Software*, doi:10.1016/j.envsoft.2008.12.011, 2009
- Grossart, H. P., Frindte, K., Dziallas, C., Eckert, W., & Tang, K. W.: Microbial methane production in oxygenated water column of an oligotrophic lake. *Proceedings of the National Academy of Sciences*, 108(49), 19657-19661, doi: 10.1073/pnas.1110716108, 2011
- 450 Günthel, M., Donis, D., Kirillin, G., Ionescu, D., Bizic, M., McGinnis, D. F., Grossart, H. P., & Tang, K. W.: Contribution of oxic methane production to surface methane emission in lakes and its global importance. *Nature communications*, 10(1), doi: 10.1038/s41467-019-13320-0, 2019
- Hama, T., Miyazaki, T., Ogawa, Y., Iwakuma, T., Takahashi, M., Otsuki, A., & Ichimura, S.: Measurement of photosynthetic production of a marine phytoplankton population using a stable ¹³C isotope. *Marine Biology*, 73(1), 31-36, doi: 10.1007/BF00396282, 1983
- 455 Hofmann, H., Federwisch, L., & Peeters, F.: Wave-induced release of methane: littoral zones as source of methane in lakes. *Limnology and Oceanography*, 55(5), 1990-2000, doi: 10.4319/lo.2010.55.5.1990 2010
- Klindworth, A., Pruesse, E., Schweer, T., Peplies, J., Quast, C., Horn, M., & Glöckner, F. O.: Evaluation of general 16S ribosomal RNA gene PCR primers for classical and next-generation sequencing-based diversity studies. *Nucleic acids research*, 41(1), doi: 10.1093/nar/gks808, 2013
- 460 Klintzsch, T., Langer, G., Nehrke, G., Wieland, A., Lenhart, K., & Keppler, F.: Methane production by three widespread marine phytoplankton species: release rates, precursor compounds, and potential relevance for the environment. *Biogeosciences*, 16(20), 4129-4144, doi: 10.5194/bg-16-4129-2019, 2019
- 465 Kosten, S., Huszar, V. L., Bécares, E., Costa, L. S., van Donk, E., Hansson, L. A., Jeppesen, E., Kruk, C., Lacerot, G., Mazzeo, N., De Meester, L., Moss, B., Lurling, M., Noges, T., Romo, S., & Scheffer, M.: Warmer climates boost cyanobacterial dominance in shallow lakes. *Global Change Biology*, 18(1), 118-126, doi: 10.1111/j.1365-2486.2011.02488.x, 2012
- Kozich, J. J., Westcott, S. L., Baxter, N. T., Highlander, S. K., & Schloss, P. D.: Development of a dual-index sequencing strategy and curation pipeline for analyzing amplicon sequence data on the MiSeq Illumina sequencing platform. *Applied and environmental microbiology*, AEM-01043, doi: 10.1128/aem.01043-13, 2013
- 470 Lehner, B., Döll, P.: Development and validation of a global database of lakes, reservoirs and wetlands. *Journal of Hydrology*, 296: 1-22, doi: 10.1016/j.jhydrol.2004.03.028, 2004
- Lenhart, K., Klintzsch, T., Langer, G., Nehrke, G., Bunge, M., Schnell, S., & Keppler, F.: Evidence for methane production by the marine algae *Emiliania huxleyi*. *Biogeosciences*, 13(10), 3163-3174, doi:10.5194/bg-13-3163-2016, 2016
- 475 Levine, R. L., Mosoni, L., Berlett, B. S., & Stadtman, E. R.: Methionine residues as endogenous antioxidants in proteins. *Proceedings of the National Academy of Sciences*, 93(26), 15036-15040, doi: 10.1073/pnas.93.26.15036, 1996
- Lewis Jr, W. M.: Tropical limnology. *Annual review of ecology and systematics*, 18(1), 159-184, doi: 10.1146/annurev.es.18.110187.001111, 1987
- 480 Martinez-Cruz, K., Sepulveda-Jauregui, A., Greene, S., Fuchs, A., Rodriguez, M., Pansch, N., Gonsioreczyk, T., & Casper, P.: Diel variation of CH₄ and CO₂ dynamics in two contrasting temperate lakes. *Inland Waters*, 1-15, doi: 10.1080/20442041.2020.1728178, 2020
- McGinnis, D. F., Greinert, J., Artemov, Y., Beaubien, S. E., & Wüest, A. N. D. A.: Fate of rising methane bubbles in stratified waters: How much methane reaches the atmosphere?. *Journal of Geophysical Research: Oceans*, 111(C9), doi: 10.1029/2005JC003183, 2006
- 485 Mohr, W., Grosskopf, T., Wallace, D. W., & LaRoche, J.: Methodological underestimation of oceanic nitrogen fixation rates. *PLoS one*, 5(9), e12583, doi: 10.1371/journal.pone.0012583, 2010



- Montoya, J. P., Voss, M., Kahler, P., & Capone, D. G.: A Simple, High-Precision, High-Sensitivity Tracer Assay for N (inf2) Fixation. *Appl. Environ. Microbiol.*, 62(3), 986-993. doi: 10.1128/aem.62.3.986-993.1996, 1996
- 490 Morana, C., Borges, A. V., Roland, F. A. E., Darchambeau, F., Descy, J. P., & Bouillon, S.: Methanotrophy within the water column of a large meromictic tropical lake (Lake Kivu, East Africa). *Biogeosciences*, 12(7), 2077-2088, doi: 10.5194/bg-12-2077-2015, 2015
- Mountfort, D. O. & Asher, R. A. Effect of inorganic sulfide on the growth and metabolism of *Methanosarcina barkeri* strain DM. *Appl. Environ. Microbiol.* 37, 670–675 (1979).
- 495 Morana, C., Sarmiento, H., Descy, J. P., Gasol, J. M., Borges, A. V., Bouillon, S., & Darchambeau, F.: Production of dissolved organic matter by phytoplankton and its uptake by heterotrophic prokaryotes in large tropical lakes. *Limnology and Oceanography*, 59(4), 1364-1375. doi:10.4319/lo.2014.59.4.1364, 2014
- Mugidde, R., Hecky, R. E., Hendzel, L. L., & Taylor, W. D.: Pelagic nitrogen fixation in lake Victoria (East Africa). *Journal of Great Lakes Research*, 29, 76-88, doi: 10.1016/S0380-1330(03)70540-1, 2003
- 500 Murase, J., & Sugimoto, A: Inhibitory effect of light on methane oxidation in the pelagic water column of a mesotrophic lake (Lake Biwa, Japan). *Limnology and oceanography*, 50(4), 1339-1343, doi: doi.org/10.4319/lo.2005.50.4.1339, 2005
- Peeters, F., Fernandez, J. E., & Hofmann, H.: Sediment fluxes rather than oxic methanogenesis explain diffusive CH₄ emissions from lakes and reservoirs. *Scientific reports*, 9(1), 1-10, doi: doi.org/10.1038/s41598-018-36530-w, 2019
- 505 Petrillo, E., Herz, M. A. G., Fuchs, A., Reifer, D., Fuller, J., Yanovsky, M. J., Simpson, C., Brown, J. W. S., Barta, A., Kalyna, M., & Kornblihtt, A. R.: A chloroplast retrograde signal regulates nuclear alternative splicing. *Science*, 344(6182), 427-430, doi: 10.1126/science.1250322, 2014
- Repine, J. E., Eaton, J. W., Anders, M. W., Hoidal, J. R., & Fox, R. B.: Generation of hydroxyl radical by enzymes, chemicals, and human phagocytes in vitro: detection with the anti-inflammatory agent, dimethyl sulfoxide. *The Journal of clinical investigation*, 64(6), 1642-1651, doi: 10.1172/jci109626, 1979
- 510 Sarmiento, H., Romera-Castillo, C., Lindh, M., Pinhasi, J., Sala, M. M., Gasol, J. M., Marassé, C., & Taylor, G. T.: Phytoplankton species-specific release of dissolved free amino acids and their selective consumption by bacteria. *Limnology and Oceanography*, 58(3), 1123-1135, doi: 10.4319/lo.2013.58.3.1123, 2013
- Tang, K. W., McGinnis, D. F., Ionescu, D., & Grossart, H. P.: Methane production in oxic lake waters potentially increases aquatic methane flux to air. *Environmental science & technology Letters*, 3(6), 227-233, doi: 10.1021/acs.estlett.6b00150, 2016
- 515 Tolar, B. B., Powers, L. C., Miller, W. L., Wallsgrove, N. J., Popp, B. N., & Hollibaugh, J. T.: Ammonia oxidation in the ocean can be inhibited by nanomolar concentrations of hydrogen peroxide. *Frontiers in Marine Science*, 3, 237, doi: 10.3389/fmars.2016.00237, 2016
- 520 Vollenweider R.A.: Calculations models of photosynthesis-depth curves and some implications regarding day rate estimates in primary production measurements. *Memorie dell'Istituto Italiano di Idrobiologia*, 18, 425–457, 1965
- Wanninkhof, R.: Relationship between wind speed and gas exchange over the ocean. *Journal of Geophysical Research: Oceans*, 97(C5), 7373-7382, doi: 10.1029/92JC00188, 1992
- 525 Yao, M., Henny, C., & Maresca, J. A.: Freshwater bacteria release methane as a byproduct of phosphorus acquisition. *Applied and environmental microbiology*, 82(23) 6994-7003, doi: 10.1128/aem.02399-16, 2016
- Yvon-Durocher, G., Allen, A. P., Bastviken, D., Conrad, R., Gudasz, C., St-Pierre, A., Thanh-Duc, N., & Del Giorgio, P. A.: Methane fluxes show consistent temperature dependence across microbial to ecosystem scales. *Nature*, 507, 488-491, doi: 10.1038/nature13164, 2014



10. Figures

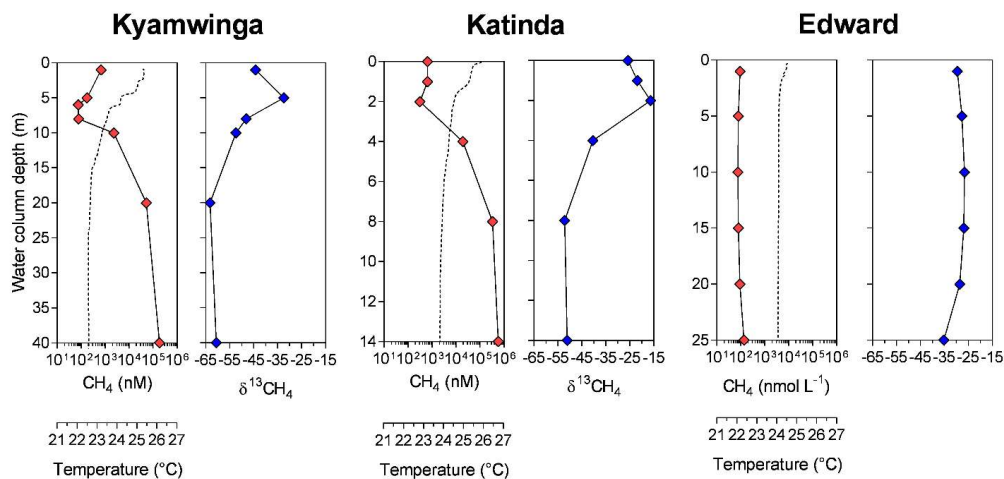


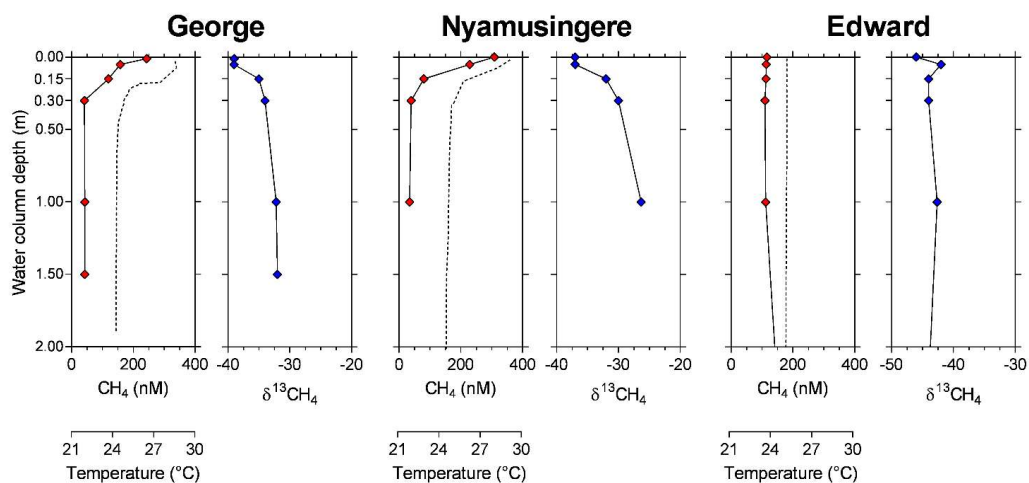
Figure 1. Depth profile. Depth profile of the temperature (°C ; dashed line), CH₄ concentration (nmol L⁻¹ ; red symbols) and stable isotope carbon composition of CH₄ (δ¹³C-CH₄, ‰ ; blue symbols) in Lake Kyamwinda (left), Lake Katinda (middle), and Lake Edward (right).

535

540

545

550



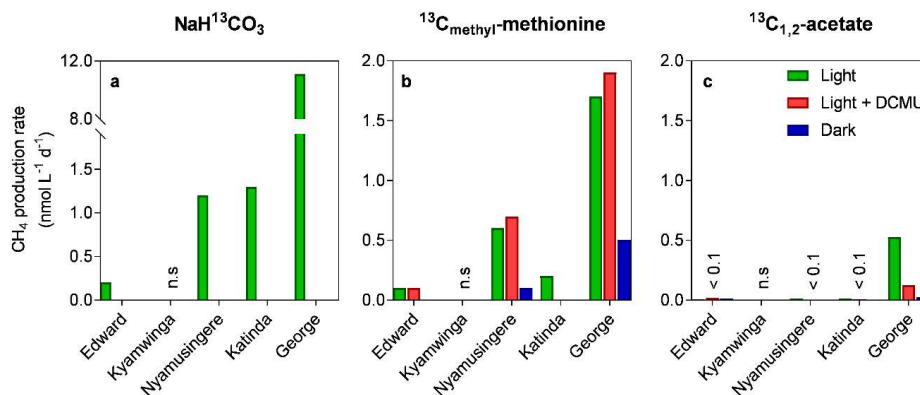
555

Figure 2. Depth profile, focus on the surface. Depth profile of the temperature (°C ; dashed line), CH₄ concentration (nmol L⁻¹ ; red symbols) and stable isotope carbon composition of CH₄ (δ¹³C-CH₄, ‰ ; blue symbols) in Lake George (left), Lake Nyamusingere (middle), and the surface waters (0-2 m) of Lake Edward (right).

560

565

570

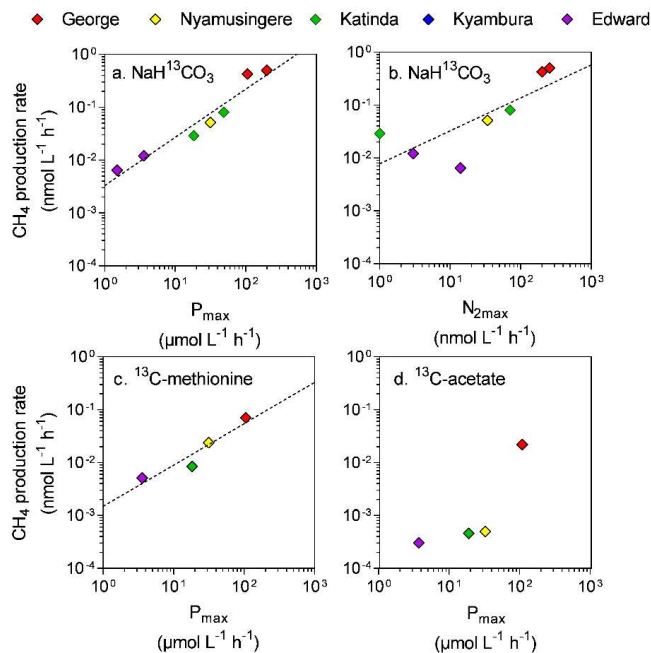


575

Figure 3. Tracer experiments show CH₄ production in well-oxygenated surface waters. CH₄ production rates (nmol L⁻¹ d⁻¹) from dissolved inorganic carbon (a), the methyl group of methionine (b) and acetate (c) measured in the surface waters (0.3 m) of a variety of African tropical lakes. Green, grey and dark bars respectively represent rates measured under light, light in presence of a photosynthesis inhibitor (DCMU), or darkness. Values showed for L. Edward, L. George and L. Katinda are the average of 2017 and 2018 sampling campaign measurement. n.s. = not significant, < 0.1 = below 0.1 nmol L⁻¹ d⁻¹.

585

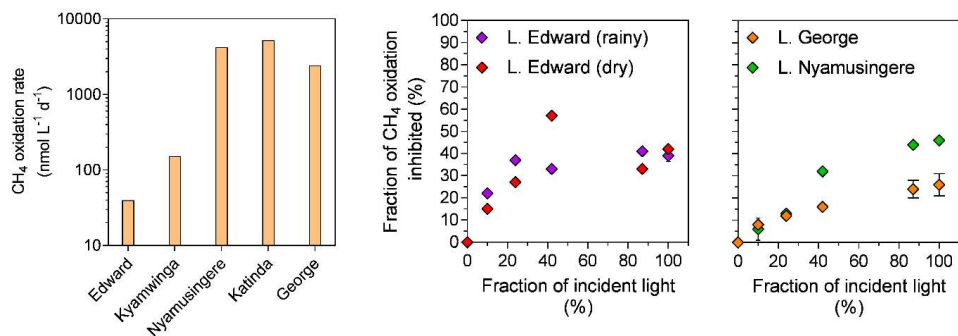
590



595 **Figure 4. Direct link between CH_4 production and phytoplankton metabolism.** Relationship between the maximum
photosynthetic activity (P_{max} , $\mu\text{mol C L}^{-1} \text{h}^{-1}$) or maximum nitrogen fixation rates ($N_{2\text{max}}$, $\text{nmol L}^{-1} \text{h}^{-1}$) and surface CH_4
production rates ($\text{nmol C L}^{-1} \text{h}^{-1}$) from dissolved inorganic carbon (a, b), methyl group of methionine (c), and acetate (d).

600

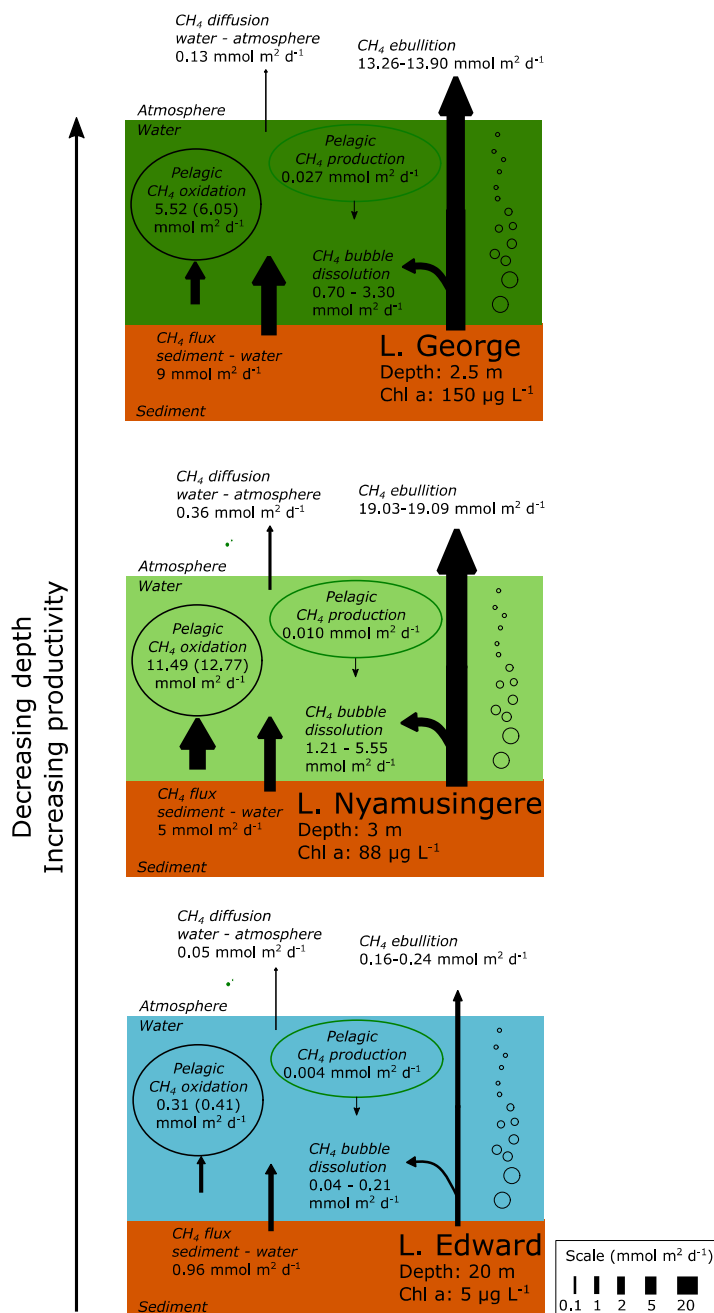
605



610 **Figure 5. Light inhibition patterns of CH₄ oxidation in surface waters.** Left panel: CH₄ oxidation rates (nmol L⁻¹ d⁻¹) measured in the surface waters (0.3 m) in the dark of a variety of African tropical lakes. Right panel: relationship between illumination (fraction of incident sunlight irradiance, %) and CH₄ oxidation inhibition (fraction of CH₄ oxidation in the dark inhibited at a given irradiance, %) in Lake Edward, Lake George and Lake Nyamusingere. Symbols represent the mean, and error bars represent the maximum and minimum of duplicate experiments

615

620



625

Figure 6. Epilimnetic CH_4 production is a marginal source of CH_4 compared to sedimentary sources and CH_4 sinks in several contrasting African lakes. Summary of the different CH_4 flux experimentally measured in L. Edward, L. George and L. Nyamusingere. Values of CH_4 oxidation in brackets are values not considering CH_4 photoinhibition. Pelagic CH_4 production are values determined from $\text{NaH}^{13}\text{CO}_3$ (~5% final enrichment) and ^{13}C -acetate (99% final enrichment), as described in the methods section. ^{13}C -labelling experiment carried out under constant light irradiance. CH_4 flux at the water-air and sediment-water interface were determined experimentally as described in the Methods. CH_4 bubble dissolution and CH_4 ebullition flux

630



were determined using the SiBu-GUI software (Greinert & McGinnis 2009); minimum and maximum represents the values obtained from two extreme bubble-size scenarios considering a release of many small (3 mm diameter) bubbles or fewer large (10 mm) bubbles.

635

640

645

650

655